

The relation between the QED charge renormalized in $\overline{\text{MS}}$ and on-shell schemes at four loops, the QED on-shell β -function at five loops and asymptotic contributions to the muon anomaly at five and six loops

P.A. Baikov^a, K.G. Chetyrkin^{b,1}, J.H. Kühn^b and C. Sturm^c

^a *Skobeltsyn Institute of Nuclear Physics, Lomonosov Moscow State University,
1(2), Leninskie gory, Moscow 119234, Russian Federation*

^b *Institut für Theoretische Teilchenphysik, Universität Karlsruhe,
D-76128 Karlsruhe, Germany*

^c *Max-Planck-Institut für Physik (Werner-Heisenberg-Institut), Föhringer Ring 6,
D-80805 München, Germany*

Abstract

In this paper we compute the four-loop corrections to the QED photon self-energy $\Pi(Q^2)$ in the two limits of $q = 0$ and $Q^2 \rightarrow \infty$. These results are used to explicitly construct the conversion relations between the QED charge renormalized in on-shell(OS) and $\overline{\text{MS}}$ scheme. Using these relations and results of Baikov et al. [1] we construct the momentum dependent part of $\Pi(Q^2, m, \alpha)$ at large Q^2 at five loops in both $\overline{\text{MS}}$ and OS schemes. As a direct consequence we arrive at the full result for the QED β -function in the OS scheme at five loops. These results are applied, in turn, to analytically evaluate a class of asymptotic contributions to the muon anomaly at five and six loops.

¹Permanent address: Institute for Nuclear Research, Russian Academy of Sciences, Moscow 117312, Russia.

1 Introduction

Quantum electrodynamics (QED) is one of the best tested and established quantum field theories. The study of its input parameters and properties is thus a challenge for each theoretician and experimentalist. For example the anomalous magnetic moment of the muon a_μ has been measured with impressing accuracy at the level of 0.5 parts per million [2, 3]: $a_\mu^{\text{exp}} = 116592089(63) \cdot 10^{-11}$. Also from theory side the anomalous magnetic moment has been studied in great detail through the computation of higher order corrections. In general higher order corrections to a_μ^{theo} are classified into three classes: pure QED, electroweak and hadronic contributions, where sample diagrams are depicted in Fig. 1.

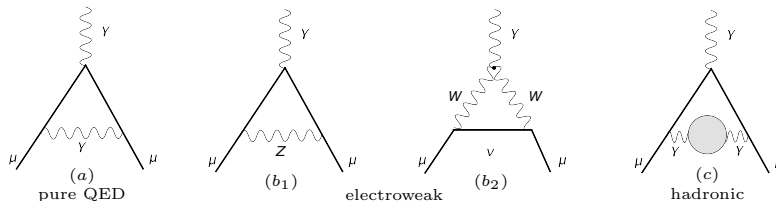


Figure 1: Sample diagrams for the classification into: pure QED contributions (a), electroweak corrections (b₁), (b₂), and hadronic contributions (c).

Within this work we consider higher order corrections to the pure QED part. Recently the complete tenth order QED contribution has been determined numerically in Ref. [4]. We refer to the reviews [5–7] and references therein for a discussion of the lower order QED corrections, the electroweak and hadronic contributions.

In QED diagrams with internal fermion loops arise starting from two-loop order, where the fermion type of the internal loop can be in general different from the external muon. In the case that the internal fermion loop consists of an electron, logarithmic contributions of the type $\ln(M_\mu/M_e)$ arise, where M_μ is the mass of the muon and M_e the mass of the electron. In view of the large mass ratio $M_\mu/M_e \sim 200$ one expects these logarithms to play a dominant role. These logarithmically enhanced contributions arise on the one hand from the insertion of the electron vacuum polarization (eVP) into the first order muon vertex diagram, shown in Fig. 1(a), but they can on the other hand also appear through light-by-light (LBL) scattering diagrams. Examples for both diagram types are shown in Fig. 2.

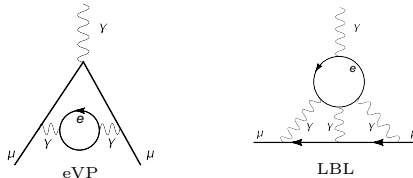


Figure 2: Example diagrams leading to dominant logarithmic contributions from electron vacuum polarization insertions and light-by-light scattering diagrams.

It has been demonstrated in Ref. [8], that the asymptotic part of the anomalous magnetic moment of the muon, a_μ^{asympt} , which contains these logarithmic contributions originating from the electron vacuum polarization function insertions, as well as the mass independent term can be obtained with the help of the electron vacuum polarization function in the asymptotic limit $M_e \rightarrow 0$. This technique has been applied in order to derive a_μ^{asympt} up to three-loop and four-loop order in Refs. [8–11]. A similar technique has also been applied in Ref. [12].

At five-loop level all diagrams contributing to a_μ^{theo} can be decomposed into six supersets, which can be further subdivided into 32 gauge invariant subsets [13]. These supersets have been computed numerically in Ref. [4]. For a few subsets also analytical results were obtained in Refs. [14, 15].

In this work we compute analytically the asymptotic limit of the photon propagator with massive electron loops and photon exchanges at four-loop order in two renormalization schemes: the $\overline{\text{MS}}$ -one and the classical on-shell scheme. The calculation is then employed for the derivation of the $\overline{\text{MS}}$ -on-shell relation of the fine structure constant α at four-loop order. This relation allows the conversion of observables, conveniently computed in the $\overline{\text{MS}}$ scheme, into the on-shell(OS) scheme or vice versa. These conversion relations combined with the recently published QED β -function in the $\overline{\text{MS}}$ scheme at five loops [1] are then used to derive the complete five-loop contribution to the QED β -function in the OS scheme as well as the *momentum-dependent* part of the polarization function in both the $\overline{\text{MS}}$ and OS scheme at five loops. These new four-loop and five-loop results are subsequently used to determine analytically a_μ^{asympt} at five loops as well as some genuinely six-loop contributions to a_μ^{asympt} . This will constitute a new analytical result for several gauge invariant subclasses of the five-loop QED muon anomaly and will serve as a check for some already known numerical results.

The outline of the paper is as follows: in Section 2 we introduce our notations and conventions. In Section 3 we discuss the methods of calculation and present the results for the vacuum polarization function for small and large Q^2 in $\overline{\text{MS}}$ and on-shell scheme. In the next Section we use these results to derive the conversion formulas between the QED charge, renormalized in $\overline{\text{MS}}$ and on-shell schemes. In Section 5 the polarization operator at five loops is discussed. In the following Section 6 we derive the complete five-loop contribution to the QED β -function in the OS scheme as well as the *momentum-dependent* part of the polarization function in both $\overline{\text{MS}}$ and OS schemes at five loops. In Sections 7 and 8 we analytically compute *all* asymptotic contributions to the muon anomaly at five loops and logarithmically enhanced ones at six loops respectively. Finally in Section 9 we close with a brief summary and our conclusions.

2 Notation and generalities

We consider QED with N identical fermions with mass m . The $\overline{\text{MS}}$ renormalized photon propagator $\overline{D}_R^{\mu\nu}$ is related to the photon polarization function $\overline{\Pi}(-q^2/\mu^2, \overline{m}/\mu, \overline{\alpha})$ in the

standard way:

$$\overline{D}_R^{\mu\nu}(-q^2, \overline{m}, \overline{\alpha}, \mu) = \frac{-g_{\mu\nu}}{-q^2} \frac{1}{1 + \overline{\Pi}(\frac{-q^2}{\mu^2}, \frac{\overline{m}}{\mu}, \overline{\alpha})} + q^\mu q^\nu \text{ terms}, \quad (1)$$

where $\overline{\alpha} \equiv \alpha^{\overline{\text{MS}}}(\mu)$, $\overline{m} \equiv \overline{m}^{\overline{\text{MS}}}(\mu)$ and μ are the running coupling constant, the fermion mass and normalization scale in $\overline{\text{MS}}$ scheme respectively. The symbol q denotes the external Minkowskian momentum of the polarization function. At four-loop order the appearing self-energy diagrams can be classified into four classes: singlet and non-singlet type diagrams, where the non-singlet ones can be again decomposed with respect to the number of inserted closed fermion loops. Some example diagrams are shown in Fig. 3.

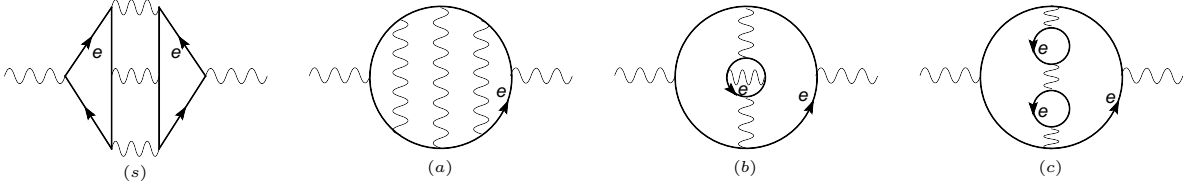


Figure 3: The four diagram classes arising in the computation of the four-loop vacuum polarization function are shown. Only one representative for each class is given. Class (s) are singlet type diagrams, whereas class (a), (b) and (c) are non-singlet type diagrams, which are decomposed according to the number of inserted fermion loops.

As is well-known the $\overline{\text{MS}}$ renormalized photon self-energy does not have any power-not suppressed terms of the type $\ln(\overline{m}^2)$ in the limit of large $Q^2 \equiv -q^2$. They appear only at order $\mathcal{O}(\overline{m}^4/Q^4)$ of the large Q asymptotic expansion (see, e.g. Ref. [16]). This allows to define the *asymptotic* part of the polarization function $\overline{\Pi}$ in the limit $\overline{m} \rightarrow 0$ as follows:

$$\overline{\Pi}^{\text{asympt}}\left(\frac{-q^2}{\mu^2}, \overline{\alpha}\right) \equiv \overline{\Pi}\left(\frac{Q^2}{\mu^2}, \frac{\overline{m}}{\mu} = 0, \overline{\alpha}\right). \quad (2)$$

The running of the coupling constant $\overline{\alpha}(\mu)$ is governed by the corresponding evolution equation of the form:

$$\mu^2 \frac{d}{d\mu^2} \ln \overline{\alpha} = \overline{\beta}(\overline{\alpha}). \quad (3)$$

The evolution equation for the polarization function can be directly obtained from the fundamental concept of the *scheme-invariant* charge [17, 18], defined through

$$\frac{\overline{\alpha}}{1 + \overline{\Pi}(\frac{-q^2}{\mu^2}, \frac{\overline{m}}{\mu}, \overline{\alpha})}. \quad (4)$$

For the case of the asymptotic polarization function the evolution equation assumes the following, particularly simple form:

$$\left\{ \mu^2 \frac{\partial}{\partial \mu^2} + \overline{\beta}(\overline{\alpha}) \left(\overline{\alpha} \frac{\partial}{\partial \overline{\alpha}} - 1 \right) \right\} (1 + \overline{\Pi}^{\text{asympt}}(Q^2/\mu^2, \overline{\alpha})) = 0. \quad (5)$$

Recently the QED β -function, as defined in the $\overline{\text{MS}}$ -scheme, has been evaluated to five-loop order [1]. For convenience of the reader we provide the corresponding result below²:

$$\begin{aligned}
\overline{\beta}(\overline{\alpha}) &= \frac{4N}{3} \frac{\overline{\alpha}}{4\pi} + 4N \left(\frac{\overline{\alpha}}{4\pi} \right)^2 - \left(\frac{\overline{\alpha}}{4\pi} \right)^3 \left[2N + \frac{44}{9} N^2 \right] \\
&+ \left(\frac{\overline{\alpha}}{4\pi} \right)^4 \left[-46N + \frac{760}{27} N^2 - \frac{832}{9} \zeta_3 N^2 - \frac{1232}{243} N^3 \right] \\
&+ \left(\frac{\overline{\alpha}}{4\pi} \right)^5 \left(N \left[\frac{4157}{6} + 128\zeta_3 \right] + N^2 \left[-\frac{7462}{9} - 992\zeta_3 + 2720\zeta_5 \right] \right. \\
&+ \left. N^3 \left[-\frac{21758}{81} + \frac{16000}{27} \zeta_3 - \frac{416}{3} \zeta_4 - \frac{1280}{3} \zeta_5 \right] + N^4 \left[\frac{856}{243} + \frac{128}{27} \zeta_3 \right] \right). \quad (6)
\end{aligned}$$

Traditionally in calculations of leptonic(ℓ) anomalies a_ℓ the classical OS scheme is employed. In this subtraction scheme the QED is parametrized with two variables, namely, the fine structure constant $\alpha \equiv \alpha^{OS}$, equal to the invariant charge (4) at zero momentum transfer, and the pole mass M of the fermion. The corresponding normalization condition for the OS polarization function $\Pi(-q^2/M^2, \alpha) \equiv \Pi^{OS}(-q^2/M^2, \alpha)$ is:

$$\Pi(-q^2 = 0, M, \alpha) \equiv 0. \quad (7)$$

The *asymptotic* polarization function $\Pi^{asympt}(Q^2/M^2, \alpha)$ is obtained from $\Pi(Q^2/M^2, \alpha)$ by discarding in every order of perturbation theory all power suppressed terms in the limit of $M \rightarrow 0$. Finally, according to Ref. [8] one obtains the asymptotic part of the muon anomaly (related to the vacuum polarization diagrams) through the relation:

$$a_\mu^{\text{asympt}} = \frac{\alpha}{\pi} \int_0^1 dx (1-x) \left[d_R^{\text{asympt}} \left(\frac{x^2 M_\mu^2}{1-x M_e^2}, \alpha \right) - 1 \right], \quad (8)$$

where

$$d_R^{\text{asympt}}(Q^2/M^2, \alpha) = \frac{1}{1 + \Pi^{\text{asympt}}(Q^2/M^2, \alpha)}. \quad (9)$$

3 The polarization function at four loops

The asymptotic limit $\overline{m} \rightarrow 0$ requires the computation of massless propagators, whereas the limit $q^2 \rightarrow 0$ leads to the evaluation of massive tadpole diagrams. The perturbative expansion of the vacuum polarization function in the fine structure constant in the two cases is conveniently defined by:

$$\overline{\Pi}(Q^2, \overline{m}^2 = 0, \overline{\alpha}) = \sum_i \overline{\Pi}^{(i)}(\ell_{\mu Q}) \left(\frac{\overline{\alpha}(\mu)}{\pi} \right)^i \quad (10)$$

²Note, please, that the function $\overline{\beta}(\overline{\alpha})$ is related to $\beta^{QED}(A)$ as given in Eq. (4.7) of [1] as follows: $\overline{\beta}(\overline{\alpha}) \equiv (\beta^{QED}(A)/A)|_{A=\overline{\alpha}/(4\pi)}$.

and

$$\overline{\Pi}(Q^2 = 0, \overline{m}^2, \overline{\alpha}) = \sum_i \overline{\Pi}^{(i)}(q = 0, \ell_{\mu m}) \left(\frac{\overline{\alpha}(\mu)}{\pi} \right)^i, \quad (11)$$

where $\ell_{\mu Q} = \ln(\mu^2/Q^2)$ and $\ell_{\mu m} = \ln(\mu^2/\overline{m}^2)$. In both cases the computation has been performed with FORM [19–21] based programs. The four-loop QED diagrams contributing to the electron polarization function have been generated with the program QGRAF [22].

The four-loop massless propagators can be reduced to 28 master integrals. The reduction of four-loop massless propagators has been done by evaluating sufficiently many terms of the $1/D$ expansion [23] of the corresponding coefficient functions [24]. The master integrals are known analytically from [25, 26].

In the low Q^2 limit all appearing tadpole diagrams have been reduced to master integrals with the help of Laporta's algorithm [27, 28]. The arising polynomials in the space-time dimension $d = 4 - 2\varepsilon$ have been simplified with the program FERMAT [29]. The remaining master integrals are known analytically to sufficient high order in ε and have been taken from Refs. [30–38].

For the large Q^2 limit our result, renormalized completely in the $\overline{\text{MS}}$ scheme, reads:

$$\overline{\Pi}^{(1)}(\ell_{\mu Q}) = N \left[\frac{5}{9} + \frac{1}{3} \ell_{\mu Q} \right], \quad (12)$$

$$\overline{\Pi}^{(2)}(\ell_{\mu Q}) = N \left[\frac{55}{48} - \zeta_3 + \frac{1}{4} \ell_{\mu Q} \right], \quad (13)$$

$$\begin{aligned} \overline{\Pi}^{(3)}(\ell_{\mu Q}) &= N \left[-\frac{143}{288} - \frac{37}{24} \zeta_3 + \frac{5}{2} \zeta_5 - \frac{1}{32} \ell_{\mu Q} \right] \\ &+ N^2 \left[-\frac{3701}{2592} + \frac{19}{18} \zeta_3 - \frac{11}{24} \ell_{\mu Q} + \frac{1}{3} \zeta_3 \ell_{\mu Q} - \frac{1}{24} \ell_{\mu Q}^2 \right], \end{aligned} \quad (14)$$

$$\begin{aligned} \overline{\Pi}^{(4)}(\ell_{\mu Q}) &= N \left[-\frac{31}{768} + \frac{13}{32} \zeta_3 + \frac{245}{32} \zeta_5 - \frac{35}{4} \zeta_7 - \frac{23}{128} \ell_{\mu Q} \right] \\ &+ N^2 \left[-\frac{7505}{41472} + \frac{11}{8640} \pi^4 + \frac{1553}{216} \zeta_3 - \zeta_3^2 - \frac{125}{18} \zeta_5 - \frac{29}{192} \ell_{\mu Q} \right. \\ &\quad \left. + \frac{19}{12} \zeta_3 \ell_{\mu Q} - \frac{5}{3} \zeta_5 \ell_{\mu Q} - \frac{1}{48} \ell_{\mu Q}^2 \right] \\ &+ N^2 \mathbf{si} \left[\frac{431}{432} - \frac{1}{360} \pi^4 - \frac{21}{16} \zeta_3 - \frac{2}{3} \zeta_3^2 + \frac{5}{4} \zeta_5 + \frac{11}{36} \ell_{\mu Q} - \frac{2}{3} \zeta_3 \ell_{\mu Q} \right] \\ &+ N^3 \left[\frac{196513}{93312} - \frac{809}{648} \zeta_3 - \frac{5}{9} \zeta_5 + \frac{151}{162} \ell_{\mu Q} - \frac{19}{27} \zeta_3 \ell_{\mu Q} + \frac{11}{72} \ell_{\mu Q}^2 \right. \\ &\quad \left. - \frac{1}{9} \zeta_3 \ell_{\mu Q}^2 + \frac{1}{108} \ell_{\mu Q}^3 \right], \end{aligned} \quad (15)$$

with ζ_n being the Riemann zeta-function defined by:

$$\zeta_n = \sum_{k=1}^{\infty} \frac{1}{k^n} \quad (16)$$

and $\ell_{\mu Q} = \ln(\frac{\mu^2}{Q^2})$. The symbol **si** is here and in the following equal one and serves only as a separator in order to display the singlet contributions, originating from diagrams of

the type as shown in Fig. 3(s), separately. As stated above, no logarithms of the type $\ln(\overline{m}^2)$ appear in this result. However, in the low $Q^2 = 0$ case the renormalized vacuum polarization function does contain logarithms of the type $\ell_{\mu m} = \ln(\frac{\mu^2}{m^2})$. In this limit our analytical result, renormalized in the $\overline{\text{MS}}$ scheme, reads:

$$\overline{\Pi}^{(1)}(q = 0, \ell_{\mu m}) = N \left[\frac{1}{3} \ell_{\mu m} \right], \quad (17)$$

$$\overline{\Pi}^{(2)}(q = 0, \ell_{\mu m}) = N \left[\frac{13}{48} - \frac{1}{4} \ell_{\mu m} \right], \quad (18)$$

$$\begin{aligned} \overline{\Pi}^{(3)}(q = 0, \ell_{\mu m}) &= N \left[\frac{97}{288} - \frac{95}{192} \zeta_3 + \frac{9}{32} \ell_{\mu m} \right] \\ &+ N^2 \left[-\frac{103}{1296} + \frac{7}{64} \zeta_3 - \frac{1}{36} \ell_{\mu m} + \frac{1}{24} \ell_{\mu m}^2 \right], \end{aligned} \quad (19)$$

$$\begin{aligned} \overline{\Pi}^{(4)}(q = 0, \ell_{\mu m}) &= \\ &N \left[-\frac{37441}{34560} + \frac{58001}{129600} \pi^4 - \frac{7549}{320} \zeta_3 + \frac{3429}{160} \zeta_5 - \frac{157}{128} \ell_{\mu m} - \frac{106}{675} \pi^4 \ln(2) \right. \\ &\left. + \frac{1919}{1080} \pi^2 \ln^2(2) - \frac{32}{135} \pi^2 \ln^3(2) - \frac{1919}{1080} \ln^4(2) + \frac{32}{225} \ln^5(2) - \frac{1919}{45} a_4 - \frac{256}{15} a_5 \right] \\ &+ N^2 \left[-\frac{2261597}{1036800} + \frac{29737}{129600} \pi^4 - \frac{123149}{10800} \zeta_3 - \frac{41}{576} \ell_{\mu m} + \frac{13}{96} \zeta_3 \ell_{\mu m} - \frac{1}{8} \ell_{\mu m}^2 \right. \\ &\left. + \frac{437}{540} \pi^2 \ln^2(2) - \frac{437}{540} \ln^4(2) - \frac{874}{45} a_4 \right] \\ &+ N^2 \text{ si} \left[\frac{2411}{5040} + \frac{2189}{17280} \pi^4 - \frac{6779}{1120} \zeta_3 - \frac{5}{12} \zeta_5 + \frac{11}{36} \ell_{\mu m} - \frac{2}{3} \zeta_3 \ell_{\mu m} \right. \\ &\left. + \frac{73}{144} \pi^2 \ln^2(2) - \frac{73}{144} \ln^4(2) - \frac{73}{6} a_4 \right] \\ &+ N^3 \left[\frac{610843}{3265920} - \frac{661}{3780} \zeta_3 + \frac{113}{1296} \ell_{\mu m} - \frac{7}{96} \zeta_3 \ell_{\mu m} + \frac{1}{108} \ell_{\mu m}^2 - \frac{1}{108} \ell_{\mu m}^3 \right], \end{aligned} \quad (20)$$

where the polylogarithm function $\text{Li}_n(1/2)$ is defined by:

$$a_n = \text{Li}_n(1/2) = \sum_{k=1}^{\infty} \frac{1}{2^k k^n}. \quad (21)$$

In the next step we convert the results of Eqs. (12)-(15) from the $\overline{\text{MS}}$ into the on-shell scheme in order to obtain the asymptotic limit of the polarization function $\Pi^{\text{asympt}}(Q^2, M^2, \alpha)$ in OS scheme. The scheme independence of the invariant charge directly leads to the relation:

$$\Pi^{\text{asympt}}(Q^2/M^2, \alpha) = \frac{\alpha}{\overline{\alpha}} \left(1 + \overline{\Pi}^{\text{asympt}}(Q^2/\mu^2, \overline{\alpha}) \right) - 1, \quad (22)$$

where it is understood that the running $\overline{\alpha}$ on the r.h.s. is converted into the on-shell coupling constant α . The corresponding conversion relation is given in the next Section 4.

In analogy to Eqs. (10) and (11) the expansion in the on-shell fine structure constant α of $\Pi^{\text{asympt}}(Q^2, M^2, \alpha)$ is defined by:

$$\Pi^{\text{asympt}}(Q^2/M^2, \alpha) = \sum_i \Pi^{\text{asympt},(i)}(\ell_{MQ}) \left(\frac{\alpha}{\pi}\right)^i. \quad (23)$$

The asymptotic limit of the polarization function in the OS scheme is given by ($\ell_{MQ} = \ln(\frac{M^2}{Q^2})$):

$$\Pi^{\text{asympt},(1)}(\ell_{MQ}) = N \left[\frac{5}{9} + \frac{1}{3} \ell_{MQ} \right], \quad (24)$$

$$\Pi^{\text{asympt},(2)}(\ell_{MQ}) = N \left[\frac{5}{24} - \zeta_3 + \frac{1}{4} \ell_{MQ} \right], \quad (25)$$

$$\begin{aligned} \Pi^{\text{asympt},(3)}(\ell_{MQ}) &= N \left[-\frac{121}{192} - \frac{5}{24} \pi^2 - \frac{99}{64} \zeta_3 + \frac{5}{2} \zeta_5 - \frac{1}{32} \ell_{MQ} + \frac{1}{3} \pi^2 \ln(2) \right] \\ &+ N^2 \left[-\frac{307}{864} - \frac{1}{9} \pi^2 + \frac{545}{576} \zeta_3 - \frac{11}{24} \ell_{MQ} + \frac{1}{3} \zeta_3 \ell_{MQ} - \frac{1}{24} \ell_{MQ}^2 \right], \quad (26) \end{aligned}$$

$$\begin{aligned} \Pi^{\text{asympt},(4)}(\ell_{MQ}) &= N \left[-\frac{71189}{34560} - \frac{157}{72} \pi^2 - \frac{59801}{129600} \pi^4 + \frac{6559}{320} \zeta_3 - \frac{1}{24} \pi^2 \zeta_3 - \frac{1603}{120} \zeta_5 \right. \\ &\quad - \frac{35}{4} \zeta_7 - \frac{23}{128} \ell_{MQ} + \frac{59}{12} \pi^2 \ln(2) + \frac{106}{675} \pi^4 \ln(2) - \frac{1559}{1080} \pi^2 \ln^2(2) + \frac{32}{135} \pi^2 \ln^3(2) \\ &\quad \left. + \frac{1559}{1080} \ln^4(2) - \frac{32}{225} \ln^5(2) + \frac{1559}{45} a_4 + \frac{256}{15} a_5 \right] \\ + N^2 &\left[\frac{3361}{900} - \frac{179}{324} \pi^2 - \frac{2161}{10800} \pi^4 + \frac{29129}{1800} \zeta_3 - \zeta_3^2 - \frac{125}{18} \zeta_5 \right. \\ &\quad + \frac{1}{12} \ell_{MQ} + \frac{19}{12} \zeta_3 \ell_{MQ} - \frac{5}{3} \zeta_5 \ell_{MQ} - \frac{1}{48} \ell_{MQ}^2 + \frac{16}{27} \pi^2 \ln(2) - \frac{53}{60} \pi^2 \ln^2(2) \\ &\quad \left. + \frac{53}{60} \ln^4(2) + \frac{106}{5} a_4 \right] \\ + N^2 \text{ si} &\left[\frac{1963}{3780} - \frac{2237}{17280} \pi^4 + \frac{5309}{1120} \zeta_3 - \frac{2}{3} \zeta_3^2 + \frac{5}{3} \zeta_5 + \frac{11}{36} \ell_{MQ} \right. \\ &\quad \left. - \frac{2}{3} \zeta_3 \ell_{MQ} - \frac{73}{144} \pi^2 \ln^2(2) + \frac{73}{144} \ln^4(2) + \frac{73}{6} a_4 \right] \\ + N^3 &\left[\frac{75259}{68040} + \frac{8}{405} \pi^2 - \frac{15109}{22680} \zeta_3 - \frac{5}{9} \zeta_5 + \frac{151}{162} \ell_{MQ} - \frac{19}{27} \zeta_3 \ell_{MQ} \right. \\ &\quad \left. + \frac{11}{72} \ell_{MQ}^2 - \frac{1}{9} \zeta_3 \ell_{MQ}^2 + \frac{1}{108} \ell_{MQ}^3 \right]. \quad (27) \end{aligned}$$

The results displayed in Eqs. (24)-(26) (as well as those in Eqs. (12)-(14), (17)-(19)) are known since long (see, e.g. [9] and references therein). Note that all terms proportional to ℓ_{MQ} in Eq. (27) follow in an easy way from renormalization group arguments as explained in [8]. In addition, in the process of constructing d_R^{asympt} one should invert the power series for $(1 + \Pi^{\text{asympt}})$, which also produces childishly-easy-to-compute factorizable fourth order

contributions to d_R^{asympt} like $\alpha^4 \Pi^{\text{asympt.}(2)} \Pi^{\text{asympt.}(2)}$ and so on (see e.g. [39] and references therein). However, to include power suppressed terms of order $(M/Q)^n$ to Π^{OS} is much less trivial even for the factorizable contributions [40, 41]. In fact, the second work also provides power suppressed contributions to the muon anomaly from factorizable diagrams of type I(a) (see Fig. 4) for the cases when leptons circulated in closed loops could be not just electrons but also muons and tau-leptons in different combinations.

4 The QED charge renormalized in $\overline{\text{MS}}$ and on-shell scheme

Let us define the conversion factor $C_{\alpha\bar{\alpha}}$, which converts the fine structure constant $\bar{\alpha}$ in $\overline{\text{MS}}$ scheme into α in OS scheme: $\alpha = C_{\alpha\bar{\alpha}}\bar{\alpha}$. The conversion factor $C_{\alpha\bar{\alpha}}$ has a perturbative expansion in $\bar{\alpha}$ defined by:

$$C_{\alpha\bar{\alpha}} = 1 + \sum_{i \geq 1} C_{\alpha\bar{\alpha}}^{(i)} \left(\frac{\bar{\alpha}(\mu)}{\pi} \right)^i. \quad (28)$$

The expansion coefficients $C_{\alpha\bar{\alpha}}^{(i)}$ can be obtained by evaluating Eq. (22) at $Q^2 = 0$ and using Eq. (7). On the r.h.s. of this equation we insert the results of Eqs. (11), (17)-(20) and expand in $\bar{\alpha}$ up to four-loop order. In addition, one should use the relation to convert the $\overline{\text{MS}}$ -mass $\overline{m}(\mu)$ to the on-shell mass M , which is known from Refs. [42, 43] to three-loop order. For the case of QED it is given in Appendix A.

The different orders $C_{\alpha\bar{\alpha}}^{(i)}$ read:

$$C_{\alpha\bar{\alpha}}^{(1)}(\ell_{\mu M}) = + N \left[-\frac{1}{3} \ell_{\mu M} \right], \quad (29)$$

$$C_{\alpha\bar{\alpha}}^{(2)}(\ell_{\mu M}) = + N \left[-\frac{15}{16} - \frac{1}{4} \ell_{\mu M} \right] + N^2 \left[\frac{1}{9} \ell_{\mu M}^2 \right], \quad (30)$$

$$C_{\alpha\bar{\alpha}}^{(3)}(\ell_{\mu M}) = + N \left[-\frac{77}{576} - \frac{5}{24} \pi^2 - \frac{1}{192} \zeta_3 + \frac{1}{32} \ell_{\mu M} + \frac{1}{3} \pi^2 \ln(2) \right] + N^2 \left[\frac{695}{648} - \frac{1}{9} \pi^2 - \frac{7}{64} \zeta_3 + \frac{73}{72} \ell_{\mu M} + \frac{5}{24} \ell_{\mu M}^2 \right] + N^3 \left[-\frac{1}{27} \ell_{\mu M}^3 \right], \quad (31)$$

$$\begin{aligned}
C_{\overline{\alpha}\alpha}^{(4)}(\ell_{\mu M}) = & \\
& + N \left[-\frac{34897}{17280} - \frac{157}{72} \pi^2 - \frac{59801}{129600} \pi^4 + \frac{6429}{320} \zeta_3 - \frac{1}{24} \pi^2 \zeta_3 - \frac{10087}{480} \zeta_5 \right. \\
& \quad + \frac{23}{128} \ell_{\mu M} + \frac{59}{12} \pi^2 \ln(2) + \frac{106}{675} \pi^4 \ln(2) - \frac{1559}{1080} \pi^2 \ln^2(2) \\
& \quad \left. + \frac{32}{135} \pi^2 \ln^3(2) + \frac{1559}{1080} \ln^4(2) - \frac{32}{225} \ln^5(2) + \frac{1559}{45} a_4 + \frac{256}{15} a_5 \right] \\
& + N^2 \left[\frac{4768247}{1036800} - \frac{179}{324} \pi^2 - \frac{8699}{43200} \pi^4 + \frac{107249}{10800} \zeta_3 + \frac{1861}{1728} \ell_{\mu M} + \frac{5}{18} \pi^2 \ell_{\mu M} \right. \\
& \quad - \frac{43}{144} \zeta_3 \ell_{\mu M} + \frac{1}{16} \ell_{\mu M}^2 + \frac{16}{27} \pi^2 \ln(2) - \frac{4}{9} \pi^2 \ell_{\mu M} \ln(2) - \frac{53}{60} \pi^2 \ln^2(2) \\
& \quad \left. + \frac{53}{60} \ln^4(2) + \frac{106}{5} a_4 \right] \\
& + N^2 \mathbf{si} \left[-\frac{2411}{5040} - \frac{2189}{17280} \pi^4 + \frac{6779}{1120} \zeta_3 + \frac{5}{12} \zeta_5 - \frac{11}{36} \ell_{\mu M} + \frac{2}{3} \zeta_3 \ell_{\mu M} \right. \\
& \quad \left. - \frac{73}{144} \pi^2 \ln^2(2) + \frac{73}{144} \ln^4(2) + \frac{73}{6} a_4 \right] \\
& + N^3 \left[-\frac{3265523}{3265920} + \frac{8}{405} \pi^2 + \frac{2201}{3780} \zeta_3 - \frac{5483}{3888} \ell_{\mu M} + \frac{4}{27} \pi^2 \ell_{\mu M} + \frac{7}{48} \zeta_3 \ell_{\mu M} \right. \\
& \quad \left. - \frac{101}{144} \ell_{\mu M}^2 - \frac{13}{108} \ell_{\mu M}^3 \right] \\
& + N^4 \left[\frac{1}{81} \ell_{\mu M}^4 \right], \tag{32}
\end{aligned}$$

with $\ell_{\mu M} = \ln(\mu^2/M^2)$. On the other hand the inverse conversion factor $C_{\overline{\alpha}\alpha}$, which allows a conversion from the $\overline{\text{MS}}$ to the on-shell scheme $\overline{\alpha} = C_{\overline{\alpha}\alpha} \alpha$ is useful as well. In analogy to Eq. (28) the perturbative expansion in α of $C_{\overline{\alpha}\alpha}$ is defined as:

$$C_{\overline{\alpha}\alpha} = 1 + \sum_{i \geq 1} C_{\overline{\alpha}\alpha}^{(i)} \left(\frac{\alpha}{\pi} \right)^i. \tag{33}$$

Proceeding like in the previous case and inverting the series obtained with the help of Eq. (22), we find:

$$\begin{aligned}
C_{\overline{\alpha}\alpha}^{(1)}(\ell_{\mu M}) = & \\
& + N \left[\frac{1}{3} \ell_{\mu M} \right], \tag{34}
\end{aligned}$$

$$\begin{aligned}
C_{\overline{\alpha}\alpha}^{(2)}(\ell_{\mu M}) = & \\
& + N \left[\frac{15}{16} + \frac{1}{4} \ell_{\mu M} \right] \\
& + N^2 \left[\frac{1}{9} \ell_{\mu M}^2 \right], \tag{35}
\end{aligned}$$

$$\begin{aligned}
C_{\bar{\alpha}\alpha}^{(3)}(\ell_{\mu M}) = & \\
& + N \left[\frac{77}{576} + \frac{5}{24} \pi^2 + \frac{1}{192} \zeta_3 - \frac{1}{32} \ell_{\mu M} - \frac{1}{3} \pi^2 \ln(2) \right] \\
& + N^2 \left[-\frac{695}{648} + \frac{1}{9} \pi^2 + \frac{7}{64} \zeta_3 + \frac{79}{144} \ell_{\mu M} + \frac{5}{24} \ell_{\mu M}^2 \right] \\
& + N^3 \left[\frac{1}{27} \ell_{\mu M}^3 \right], \tag{36}
\end{aligned}$$

$$\begin{aligned}
C_{\bar{\alpha}\alpha}^{(4)}(\ell_{\mu M}) = & \\
& + N \left[\frac{34897}{17280} + \frac{157}{72} \pi^2 + \frac{59801}{129600} \pi^4 - \frac{6429}{320} \zeta_3 + \frac{1}{24} \pi^2 \zeta_3 + \frac{10087}{480} \zeta_5 \right. \\
& \quad - \frac{23}{128} \ell_{\mu M} - \frac{59}{12} \pi^2 \ln(2) - \frac{106}{675} \pi^4 \ln(2) + \frac{1559}{1080} \pi^2 \ln^2(2) \\
& \quad \left. - \frac{32}{135} \pi^2 \ln^3(2) - \frac{1559}{1080} \ln^4(2) + \frac{32}{225} \ln^5(2) - \frac{1559}{45} a_4 - \frac{256}{15} a_5 \right] \\
& + N^2 \left[-\frac{2034497}{1036800} + \frac{179}{324} \pi^2 + \frac{8699}{43200} \pi^4 - \frac{107249}{10800} \zeta_3 + \frac{1031}{1728} \ell_{\mu M} + \frac{5}{36} \pi^2 \ell_{\mu M} \right. \\
& \quad + \frac{89}{288} \zeta_3 \ell_{\mu M} + \frac{1}{16} \ell_{\mu M}^2 - \frac{16}{27} \pi^2 \ln(2) - \frac{2}{9} \pi^2 \ell_{\mu M} \ln(2) + \frac{53}{60} \pi^2 \ln^2(2) \\
& \quad \left. - \frac{53}{60} \ln^4(2) - \frac{106}{5} a_4 \right] \\
& + N^2 \text{ si} \left[\frac{2411}{5040} + \frac{2189}{17280} \pi^4 - \frac{6779}{1120} \zeta_3 - \frac{5}{12} \zeta_5 + \frac{11}{36} \ell_{\mu M} - \frac{2}{3} \zeta_3 \ell_{\mu M} \right. \\
& \quad \left. + \frac{73}{144} \pi^2 \ln^2(2) - \frac{73}{144} \ln^4(2) - \frac{73}{6} a_4 \right] \\
& + N^3 \left[\frac{3265523}{3265920} - \frac{8}{405} \pi^2 - \frac{2201}{3780} \zeta_3 - \frac{2857}{3888} \ell_{\mu M} + \frac{2}{27} \pi^2 \ell_{\mu M} + \frac{7}{96} \zeta_3 \ell_{\mu M} \right. \\
& \quad \left. + \frac{17}{72} \ell_{\mu M}^2 + \frac{13}{108} \ell_{\mu M}^3 \right] \\
& + N^4 \left[\frac{1}{81} \ell_{\mu M}^4 \right]. \tag{37}
\end{aligned}$$

5 The polarization function at five loops

In this section we will use the recent calculation [1] of $\bar{\beta}(\bar{\alpha})$ — the QED β -function in the $\overline{\text{MS}}$ scheme — at five-loop order to find the Q -dependent part of the five-loop contribution to the asymptotic polarization function in both $\overline{\text{MS}}$ and OS schemes.

5.1 $\overline{\text{MS}}$ scheme

We start by transforming evolution equation (5) for the $\overline{\text{MS}}$ -renormalized asymptotic photon polarization into the form:

$$\mu^2 \frac{\partial}{\partial \mu^2} \overline{\Pi}^{\text{asympt}} \left(\frac{Q^2}{\mu^2}, \overline{\alpha} \right) = \overline{\beta}(\overline{\alpha}) \left(1 - \overline{\alpha}^2 \frac{\partial}{\partial \overline{\alpha}} \frac{\overline{\Pi}^{\text{asympt}} \left(\frac{Q^2}{\mu^2}, \overline{\alpha} \right)}{\overline{\alpha}} \right). \quad (38)$$

Now by direct integration of the r.h.s. of Eq. (38) one can easily construct the Q -dependent part of $\overline{\Pi}^{\text{asympt}} \left(\frac{Q^2}{\mu^2}, \overline{\alpha} \right)$ in order $\overline{\alpha}^5$:

$$\begin{aligned} \overline{\Pi}^{(5)}(\ell_{\mu Q}) = N \ell_{\mu Q} \left\{ \right. \\ & \frac{4157}{6144} + \frac{1}{8} \zeta_3 + N \left[\frac{689}{1152} + \frac{67}{96} \zeta_3 - \frac{115}{12} \zeta_5 + \frac{35}{4} \zeta_7 + \frac{13}{128} \ell_{\mu Q} \right] \\ & + N \text{ si} \left[-\frac{13}{12} - \frac{4}{3} \zeta_3 + \frac{10}{3} \zeta_5 \right] \\ & + N^2 \left[\frac{5713}{5184} - \frac{581}{72} \zeta_3 + \zeta_3^2 + \frac{125}{18} \zeta_5 + \frac{115}{576} \ell_{\mu Q} - \frac{7}{8} \zeta_3 \ell_{\mu Q} \right. \\ & \quad \left. + \frac{5}{6} \zeta_5 \ell_{\mu Q} + \frac{1}{72} \ell_{\mu Q}^2 \right] \\ & + N^2 \text{ si} \left[-\frac{149}{108} + \frac{13}{6} \zeta_3 + \frac{2}{3} \zeta_3^2 - \frac{5}{3} \zeta_5 - \frac{11}{72} \ell_{\mu Q} + \frac{1}{3} \zeta_3 \ell_{\mu Q} \right] \\ & + N^3 \left[-\frac{6131}{2916} + \frac{203}{162} \zeta_3 + \frac{5}{9} \zeta_5 - \frac{151}{324} \ell_{\mu Q} + \frac{19}{54} \zeta_3 \ell_{\mu Q} - \frac{11}{216} \ell_{\mu Q}^2 \right. \\ & \quad \left. + \frac{1}{27} \zeta_3 \ell_{\mu Q}^2 - \frac{1}{432} \ell_{\mu Q}^3 \right] \left. \right\}. \quad (39) \end{aligned}$$

5.2 OS scheme

By inspecting Eq. (22) relating the photon polarization function normalized in the $\overline{\text{MS}}$ and OS schemes one observes that the Q -dependent part of the $\mathcal{O}(\alpha^5)$ OS-normalized asymptotic polarization function is recoverable from Eq. (6), four-loop conversion relations and five-loop asymptotic $\overline{\text{MS}}$ polarization function. The result is:

$$\begin{aligned} \Pi^{(5)}(\ell_{MQ}) = N \ell_{MQ} \left\{ \right. \\ & \frac{4157}{6144} + \frac{1}{8} \zeta_3 \\ & + N \left[\frac{55}{96} + \frac{5}{96} \pi^2 + \frac{179}{256} \zeta_3 - \frac{115}{12} \zeta_5 + \frac{35}{4} \zeta_7 + \frac{13}{128} \ell_{MQ} - \frac{1}{12} \pi^2 \ln(2) \right] \\ & + N \text{ si} \left[-\frac{13}{12} - \frac{4}{3} \zeta_3 + \frac{10}{3} \zeta_5 \right] \\ & + N^2 \left[-\frac{11}{432} + \frac{1}{36} \pi^2 - \frac{17089}{2304} \zeta_3 + \zeta_3^2 + \frac{125}{18} \zeta_5 + \frac{35}{288} \ell_{MQ} \right. \\ & \quad \left. - \frac{7}{8} \zeta_3 \ell_{MQ} + \frac{5}{6} \zeta_5 \ell_{MQ} + \frac{1}{72} \ell_{MQ}^2 \right] \left. \right\} \end{aligned}$$

$$\begin{aligned}
& + N^2 \mathbf{si} \left[-\frac{149}{108} + \frac{13}{6}\zeta_3 + \frac{2}{3}\zeta_3^2 - \frac{5}{3}\zeta_5 - \frac{11}{72}\ell_{MQ} + \frac{1}{3}\zeta_3\ell_{MQ} \right] \\
& + N^3 \left[-\frac{6131}{2916} + \frac{203}{162}\zeta_3 + \frac{5}{9}\zeta_5 - \frac{151}{324}\ell_{MQ} + \frac{19}{54}\zeta_3\ell_{MQ} - \frac{11}{216}\ell_{MQ}^2 \right. \\
& \quad \left. + \frac{1}{27}\zeta_3\ell_{MQ}^2 - \frac{1}{432}\ell_{MQ}^3 \right] \Big\}. \tag{40}
\end{aligned}$$

6 The QED β -function in the OS scheme at five loops

The OS β -function,

$$\beta(\alpha) \equiv \beta^{OS}(\alpha) \equiv \sum_{i \geq 1} \beta_i \left(\frac{\alpha}{\pi} \right)^i, \tag{41}$$

describes the evolution of the asymptotic photon polarization function with respect to the change of the mass M , namely (see, e.g. [44]):

$$\left\{ M^2 \frac{\partial}{\partial M^2} + \beta(\alpha) \left(\alpha \frac{\partial}{\partial \alpha} - 1 \right) \right\} (1 + \Pi^{\text{asympt}}(\ell_{MQ}, \alpha)) = 0. \tag{42}$$

At the four-loop level $\beta(\alpha)$ is known since long [9]. One could easily check that Eq. (42) is indeed met by our four-loop result given in Eqs. (23) and (27).

For our purposes it is useful to rewrite Eq. (42) in the form:

$$\left(M^2 \frac{\partial}{\partial M^2} + \beta(\alpha) \alpha \frac{\partial}{\partial \alpha} \right) \frac{\Pi^{\text{asympt}}(\ell_{MQ}, \alpha)}{\alpha} = \frac{\beta(\alpha)}{\alpha}. \tag{43}$$

Eq. (43) demonstrates that one could construct the next $(L + 1)$ order contribution to β provided one has the polarization function Π^{asympt} in L -loops (that is up to and including the terms of order α^L) and its all logarithmic (that is proportional to ℓ_{MQ}) terms of order α^{L+1} . Thus, we have at our disposal all ingredients to find β^{OS} at five loops. The result reads:

$$\beta_1 = \frac{N}{3}, \tag{44}$$

$$\beta_2 = \frac{N}{4}, \tag{45}$$

$$\beta_3 = -\frac{N}{32} - \frac{7N^2}{18}, \tag{46}$$

$$\beta_4 = -\frac{23N}{128} + N^2 \left[\frac{1}{48} - \frac{5}{36}\pi^2 - \frac{35}{96}\zeta_3 + \frac{2}{9}\pi^2 \ln(2) \right] + N^3 \left[\frac{901}{1296} - \frac{2}{27}\pi^2 - \frac{7}{96}\zeta_3 \right], \tag{47}$$

$$\beta_5 = N \left[\frac{4157}{6144} + \frac{1}{8}\zeta_3 \right]$$

$$\begin{aligned}
& + N^2 \left[-\frac{12493}{4320} - \frac{643}{288} \pi^2 - \frac{59801}{129600} \pi^4 + \frac{73423}{3840} \zeta_3 - \frac{1}{24} \pi^2 \zeta_3 - \frac{2203}{120} \zeta_5 \right. \\
& \quad + 5 \pi^2 \ln(2) + \frac{106}{675} \pi^4 \ln(2) - \frac{1559}{1080} \pi^2 \ln^2(2) + \frac{32}{135} \pi^2 \ln^3(2) \\
& \quad \left. + \frac{1559}{1080} \ln^4(2) - \frac{32}{225} \ln^5(2) + \frac{1559}{45} a_4 + \frac{256}{15} a_5 \right] \\
& + N^3 \left[\frac{783211}{302400} - \frac{47}{81} \pi^2 - \frac{9491}{28800} \pi^4 + \frac{2222237}{134400} \zeta_3 + \frac{16}{27} \pi^2 \ln(2) - \frac{1001}{720} \pi^2 \ln^2(2) \right. \\
& \quad \left. + \frac{1001}{720} \ln^4(2) + \frac{1001}{30} a_4 \right] \\
& + N^4 \left[-\frac{203393}{204120} + \frac{8}{405} \pi^2 + \frac{493}{840} \zeta_3 \right]. \tag{48}
\end{aligned}$$

7 Contributions to the muon anomaly at five loops

Having at hand the result for the asymptotic polarization function at four-loop order in QED, one can use it in combination with Eqs. (9) and (8) to determine the full asymptotic contribution (that is coming from electron vacuum polarization insertions in the limit $M_e/M_\mu \rightarrow 0$) to the muon anomaly at five-loops. The first of the six supersets of diagrams, which contribute at five-loop order to the muon anomaly is shown in Fig. 4. It can be subdivided into ten gauge invariant subsets.

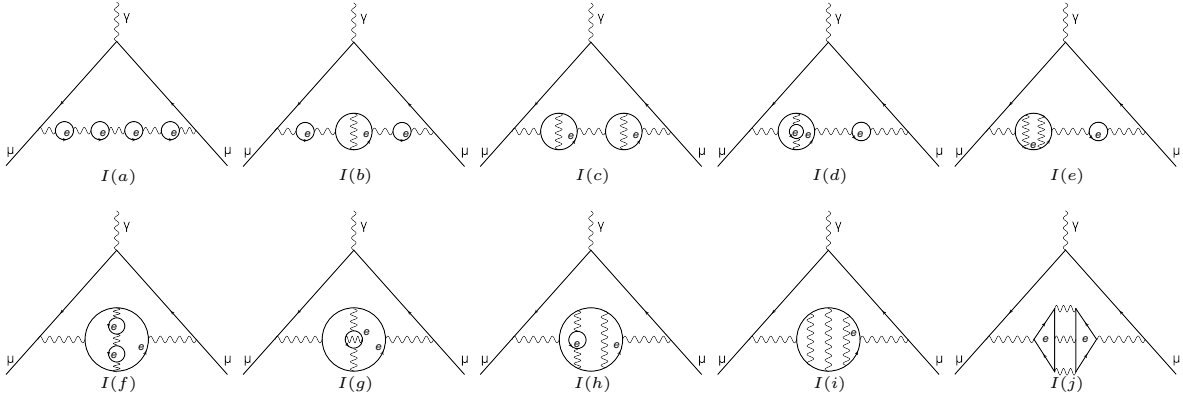


Figure 4: The ten gauge invariant subsets contributing to the muon anomaly which originate from inserting the vacuum polarization up to four-loop order into the first order QED vertex of Fig. 1(a). For each diagram class only one typical representative is shown. Wavy lines denote photons(γ), solid lines denote electrons(e) or muons (μ). The last five diagrams $\{I(f), I(g), I(h), I(i), I(j)\}$ are non-factorizable insertions of the vacuum polarization function; the first five diagrams $\{I(a), I(b), I(c), I(d), I(e)\}$ are factorizable ones.

We define the perturbative expansion of the anomalous magnetic moment of the muon

by:

$$a_\mu^{asympt} = \sum_i a_\mu^{asympt,(i)} \left(\frac{\alpha}{\pi}\right)^i, \quad i = 2, 3, \dots \quad (49)$$

The decomposition of a_μ^{asympt} into the ten subsets shown in Fig. 4 is given by:

$$\begin{aligned} a_\mu^{asympt,(5)} \Big|_{Fig. 4} &= a_\mu^{(5),\{a\}} + a_\mu^{(5),\{b\}} + a_\mu^{(5),\{c\}} + a_\mu^{(5),\{d\}} + a_\mu^{(5),\{e\}} \\ &+ a_\mu^{(5),\{f\}} + a_\mu^{(5),\{g+h\}} + a_\mu^{(5),\{i\}} + a_\mu^{(5),\{j\}}. \end{aligned} \quad (50)$$

The letters in the curly brackets denote the respective contribution of Fig. 4. Inserting the results of Eqs. (23)-(27) into Eq. (8) and integrating the different contributions of Eq. (50) we find:

$$\begin{aligned} a_\mu^{(5),\{a\}} &= \frac{64613}{26244} + \frac{317}{729} \pi^2 + \frac{2}{135} \pi^4 + \frac{100}{81} \zeta_3 + \ell_{\mu e} \left(-\frac{8609}{2187} - \frac{100}{243} \pi^2 - \frac{16}{27} \zeta_3 \right) \\ &+ \ell_{\mu e}^2 \left(\frac{634}{243} + \frac{8}{81} \pi^2 \right) - \ell_{\mu e}^3 \frac{200}{243} + \ell_{\mu e}^4 \frac{8}{81}, \end{aligned} \quad (51)$$

$$\begin{aligned} a_\mu^{(5),\{b\}} &= -\frac{439}{162} - \frac{35}{108} \pi^2 + \frac{263}{108} \zeta_3 + \frac{\pi^2}{9} \zeta_3 + \ell_{\mu e} \left(\frac{413}{108} + \frac{\pi^2}{6} - \frac{25}{9} \zeta_3 \right) \\ &+ \ell_{\mu e}^2 \left(-\frac{35}{18} + \frac{2}{3} \zeta_3 \right) + \frac{1}{3} \ell_{\mu e}^3, \end{aligned} \quad (52)$$

$$a_\mu^{(5),\{c\}} = \frac{409}{1152} + \frac{\pi^2}{48} - \frac{5}{6} \zeta_3 + \frac{1}{2} \zeta_3^2 + \ell_{\mu e} \left(-\frac{5}{12} + \frac{\zeta_3}{2} \right) + \frac{1}{8} \ell_{\mu e}^2, \quad (53)$$

$$\begin{aligned} a_\mu^{(5),\{d\}} &= -\frac{40057}{15552} - \frac{221}{648} \pi^2 + \frac{24185}{10368} \zeta_3 + \frac{2}{27} \pi^2 \zeta_3 + \ell_{\mu e} \left(\frac{3949}{1296} + \frac{7}{54} \pi^2 - \frac{1825}{864} \zeta_3 \right) \\ &+ \ell_{\mu e}^2 \left(-\frac{121}{108} + \frac{4}{9} \zeta_3 \right) + \frac{1}{9} \ell_{\mu e}^3, \end{aligned} \quad (54)$$

$$\begin{aligned} a_\mu^{(5),\{e\}} &= -\frac{3409}{3456} - \frac{8}{27} \pi^2 + \frac{25}{54} \pi^2 \ln(2) - \frac{275}{128} \zeta_3 + \frac{125}{36} \zeta_5 \\ &+ \ell_{\mu e} \left(\frac{161}{288} + \frac{5}{36} \pi^2 + \frac{33}{32} \zeta_3 - \frac{5}{3} \zeta_5 - \frac{8}{36} \pi^2 \ln(2) \right) - \frac{1}{24} \ell_{\mu e}^2, \end{aligned} \quad (55)$$

$$\begin{aligned} a_\mu^{(5),\{f\}} &= -\frac{315079}{136080} - \frac{34}{405} \pi^2 + \frac{68869}{45360} \zeta_3 + \frac{\pi^2}{27} \zeta_3 + \frac{5}{18} \zeta_5 \\ &+ \ell_{\mu e} \left(\frac{152}{81} + \frac{\pi^2}{54} - \frac{34}{27} \zeta_3 \right) + \ell_{\mu e}^2 \left(-\frac{4}{9} + \frac{2}{9} \zeta_3 \right) + \frac{1}{27} \ell_{\mu e}^3, \end{aligned} \quad (56)$$

$$\begin{aligned} a_\mu^{(5),\{g+h\}} &= -\frac{27413}{14400} - \frac{53}{5} a_4 - \frac{53}{120} \ln^4(2) + \frac{367}{1296} \pi^2 - \frac{8}{27} \pi^2 \ln(2) \\ &+ \frac{53}{120} \pi^2 \ln^2(2) + \frac{2161}{21600} \pi^4 - \frac{18127}{1800} \zeta_3 + \frac{\zeta_3^2}{2} + \frac{50}{9} \zeta_5 \\ &+ \ell_{\mu e} \left(-\frac{1}{48} + \frac{19}{12} \zeta_3 - \frac{5}{3} \zeta_5 \right) + \frac{1}{24} \ell_{\mu e}^2, \end{aligned} \quad (57)$$

$$a_\mu^{(5),\{i\}} = \frac{43357}{34560} - \frac{1559}{90} a_4 - \frac{128}{15} a_5 - \frac{1559}{2160} \ln^4(2) + \frac{16}{225} \ln^5(2) + \frac{157}{144} \pi^2$$

$$\begin{aligned}
& -\frac{59}{24}\pi^2 \ln(2) + \frac{1559}{2160}\pi^2 \ln^2(2) - \frac{16}{135}\pi^2 \ln^3(2) + \frac{59801}{259200}\pi^4 \\
& -\frac{53}{675}\pi^4 \ln(2) - \frac{6559}{640}\zeta_3 + \frac{\pi^2}{48}\zeta_3 + \frac{1603}{240}\zeta_5 + \frac{35}{8}\zeta_7 - \frac{23}{128}\ell_{\mu e}, \tag{58}
\end{aligned}$$

$$\begin{aligned}
a_\mu^{(5),\{j\}} = & -\frac{9701}{15120} - \frac{73}{12}a_4 - \frac{73}{288}\ln^4(2) + \frac{73}{288}\pi^2 \ln^2(2) + \frac{2237}{34560}\pi^4 \\
& -\frac{10327}{6720}\zeta_3 + \frac{\zeta_3^2}{3} - \frac{5}{6}\zeta_5 + \ell_{\mu e} \left(\frac{11}{36} - \frac{2}{3}\zeta_3 \right), \tag{59}
\end{aligned}$$

with $\ell_{\mu e} = \ln(M_\mu/M_e)$. Power suppressed terms of the order $\mathcal{O}(M_e/M_\mu)$ are neglected. The coefficients of the logarithmic terms $\ell_{\mu e}$ have been computed analytically in Ref. [14], except for the complete $\ell_{\mu e}$ -term in Eq. (55). For the factorizable insertions of the vacuum polarization function also the mass independent term has been determined analytically in Refs. [14, 15], except for the case $I(e)$. All the analytical results of Refs. [9, 14, 15] for Eqs. (56)-(51) are in agreement with ours. Numerical results for these ten gauge invariant subsets of diagrams which are shown in Fig. 4 have been reported in Refs. [45–48]. A comparison between the asymptotic analytical formulas of Eqs. (51)-(56) and the numerical results is shown in Table 1.

Subset	Analytical	Numerical	Ref.	Num.-ana.
$I(a)$	$20.1832 + \mathcal{O}(M_e/M_\mu)$	20.14293(23)	[45]	≈ -0.04
$I(b)$	$27.7188 + \mathcal{O}(M_e/M_\mu)$	27.69038(30)	[45]	≈ -0.03
$I(c)$	$4.81759 + \mathcal{O}(M_e/M_\mu)$	4.74212(14)	[45]	≈ -0.08
$I(d)$	$7.44918 + \mathcal{O}(M_e/M_\mu)$	7.45173(101)	[45]	≈ 0.003
$I(e)$	$-1.33141 + \mathcal{O}(M_e/M_\mu)$	-1.20841(70)	[45]	≈ 0.12
$I(f)$	$2.89019 + \mathcal{O}(M_e/M_\mu)$	2.88598(9)	[45]	≈ -0.004
$I(g) + I(h)$	$1.50112 + \mathcal{O}(M_e/M_\mu)$	1.56070(64)	[46]	≈ 0.06
$I(i)$	$0.25237 + \mathcal{O}(M_e/M_\mu)$	0.0871(59)	[47]	≈ -0.17
$I(j)$	$-1.21429 + \mathcal{O}(M_e/M_\mu)$	-1.24726(12)	[48]	≈ -0.03

Table 1: The first column shows the different gauge invariant subsets of diagrams as defined in Fig. 4. The second column contains the corresponding results of Eqs. (51)-(59) evaluated numerically, where we have used for the mass ratio $M_\mu/M_e = 206.7682843(52)$ [49]. This result is correct only up to power corrections in the small mass ratio M_e/M_μ . The third column contains the numerical result obtained in Refs. [45–48]. (Note that in Ref. [45] also a more precise value 7.45270(88) is given for $I(d)$ which was obtained using the exact sixth order spectral function.) The last column shows the difference between the numerical and asymptotic analytical results. The subsets $\{I(a), I(b), I(c), I(d), I(e)\}$ originate from Feynman diagrams with factorizable vacuum polarization insertions, whereas the subsets $\{I(f), I(g), I(h), I(i), I(j)\}$ are non-factorizable (see Fig. 4).

In general good agreement between asymptotic analytical and numerical results is found, except for the subsets $I(e)$ and $I(i)$ where we only have poor agreement. The remaining differences should arise from corrections of the order $\mathcal{O}(M_e/M_\mu)$.³ Summing up all ten

³For a discussion of the differences for subset $I(i)$ see also Section VIII of Ref. [47].

subsets one obtains $a_\mu^{asympt,(5)}|_{Fig. 4} = 62.26675 + \mathcal{O}(M_e/M_\mu)$ which is, despite the small number of diagrams, sizeable ($\approx 8\%$) compared to the complete numerical result $a_\mu^{(5)} = 753.29(1.04)$ of Ref. [4]. The reason for this is the logarithmic enhancement. Indeed, if we set to zero all Q -dependent terms in the asymptotic OS polarization function the result for $a_\mu^{asympt,(5)}|_{Fig. 4}$ would be reduced to 2.52261.

8 Contributions to the muon anomaly at six loops

The five-loop contribution to Eq. (9)

$$d_R^{asympt}(Q^2/M^2, \alpha) = \sum_{i \geq 0} d_i(\ell_{MQ}) \left(\frac{\alpha}{\pi}\right)^i$$

can be schematically represented as follows:

$$d_5 = d_5^{\text{factr}} - \Pi^{\text{asympt,(5)}} + C_5, \quad (60)$$

where

$$\begin{aligned} d_5^{\text{factr}} = & - \left(\Pi^{\text{asympt,(1)}}\right)^5 + 4 \left(\Pi^{\text{asympt,(1)}}\right)^3 \Pi^{\text{asympt,(2)}} - 3 \Pi^{\text{asympt,(1)}} \left(\Pi^{\text{asympt,(2)}}\right)^2 \\ & - 3 \left(\Pi^{\text{asympt,(1)}}\right)^2 \Pi^{\text{asympt,(3)}} + 2 \Pi^{\text{asympt,(2)}} \Pi^{\text{asympt,(3)}} + 2 \Pi^{\text{asympt,(1)}} \Pi^{\text{asympt,(4)}} \end{aligned} \quad (61)$$

and C_5 is a still unknown constant standing for Q -independent contributions missing in $\Pi^{\text{asympt,(5)}}$ as described by Eq. (40).

The corresponding result for the asymptotic contribution to the muon anomaly is rather bulky so we provide it below in numerical form only:

$$a_\mu^{asympt,(6)} = 257.245 + \frac{C_5}{2} = 246.381^{\text{factr}} + 10.8647 + \frac{C_5}{2}, \quad (62)$$

where after the second equality sign we decompose the result into two pieces: the factorizable and the genuine six-loop terms. We observe that the six-loop asymptotic contribution to the muon anomaly is almost completely saturated by factorizable terms. One could hardly expect that the constant C_5 might have any numerical relevance. Indeed, an analog of Eq. (62) at the five-loop level looks as:

$$a_\mu^{asympt,(5)} = 60.7524 + \frac{C_4 = 3.0287}{2} = 58.8374^{\text{factr}} + 1.915 + \frac{C_4 = 3.0287}{2}. \quad (63)$$

Thus, we believe that Eq. (62) with $C_5 = 0$ presents quite a good prediction for $a_\mu^{asympt,(6)}$.

To further study the size of the factorizable and non-factorizable six-loop contributions to the muon anomaly we subdivide them into several gauge invariant subsets in complete analogy to the five-loop case shown in Fig. 4. Let us start with the genuine,

Subset	N^4	N^3	N^2	N	si N^3	si N^2
Value	7.15995	7.15320	-2.73813	3.37488	-7.22943	3.14426

Table 2: The numerical values are correct up to power corrections of the order $\mathcal{O}(M_e/M_\mu)$ and the contribution coming from the unknown constant C_5 of Eq. (60). The symbol **si** labels singlet contributions, whereas the power of N denotes the number of closed fermion loops which arise in the corresponding diagrams.

non-factorizable contributions which correspond to the term $-\Pi^{\text{asympt},5} + C_5$ of Eq. (60) and which we again subdivide according to the number of fermion loops arising in the corresponding diagrams. The individual contributions to $a_\mu^{\text{asympt},(6)}\Big|_{\text{non-factr}} = 10.8647 + C_5/2$ of Eq. (62) are shown in numerical evaluated form in Table 2 and an example diagram for each of the six subsets of Table 2 is given in Fig. 5.

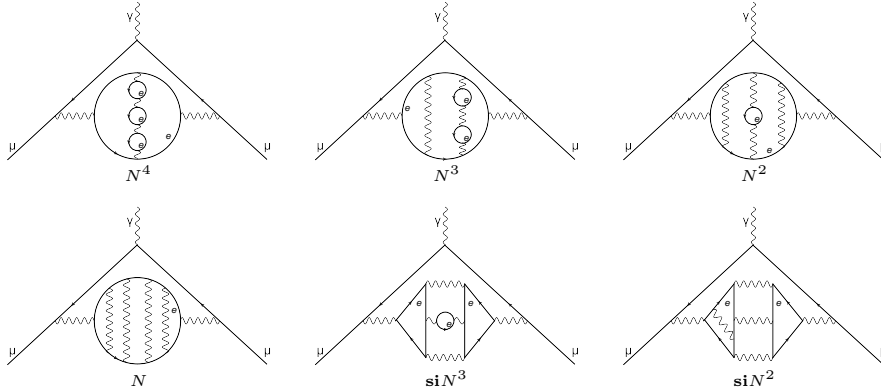


Figure 5: For each subset of Table 2 one example diagram is shown. It would be possible to subdivide these diagram classes into further subsets, however, we refrain from doing this for simplicity. The symbol **si** denotes a singlet diagram, whereas the power of N gives the number of closed fermion loops which arise in the corresponding diagrams. Wavy lines represent again photons whereas solid lines stand for electrons or muons.

The factorizable contribution of Eq. (62), $a_\mu^{\text{asympt},(6)}\Big|_{\text{factr}} = 246.381$, which originates from the terms in d_5^{factr} of Eq. (61) can also be classified into several subsets:

$$\begin{aligned}
a_\mu^{\text{asympt},(6)}\Big|_{\text{factr}} &= a_\mu^{(6),\{a\}} + a_\mu^{(6),\{b\}} + a_\mu^{(6),\{c\}} + a_\mu^{(6),\{d\}} + a_\mu^{(6),\{e\}} + a_\mu^{(6),\{f\}} \\
&+ a_\mu^{(6),\{g\}} + a_\mu^{(6),\{h\}} + a_\mu^{(6),\{i+j\}} + a_\mu^{(6),\{k\}} + a_\mu^{(6),\{l\}}, \quad (64)
\end{aligned}$$

where we have shown in Fig. 6 one typical contributing diagram for each term on the r.h.s. of Eq. (64). The letter in the upper case curly brackets denotes again from which contribution of Fig. 6 the considered term is coming. The numerical values of the factorizable contributions are shown in Table 3.

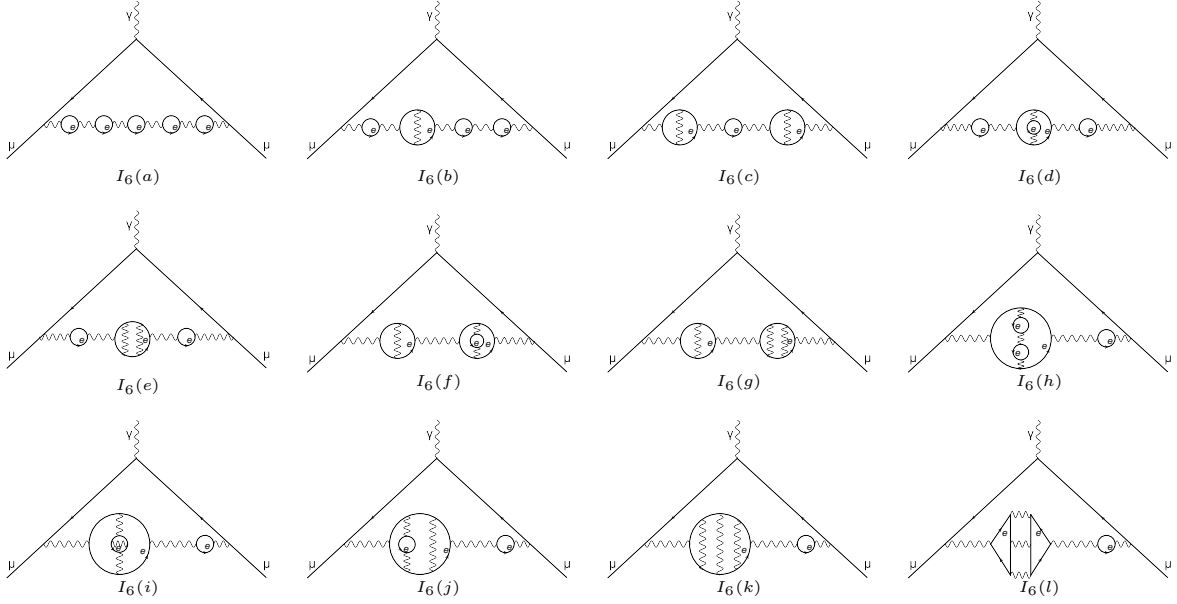


Figure 6: The different diagram classes of the factorizable six-loop contribution. For each diagram class $I_6(a)$ – $I_6(l)$ one typical representative is shown.

Subset	$I_6(a)$	$I_6(b)$	$I_6(c)$	$I_6(d)$	$I_6(e)$	$I_6(f)$
Value	58.1861	101.150	35.8953	30.6997	-5.12107	9.68427
Subset	$I_6(g)$	$I_6(h)$	$I_6(i) + I_6(j)$	$I_6(k)$	$I_6(l)$	
Value	-1.81937	15.6754	7.73424	0.68395	-6.38790	

Table 3: Numerical evaluation for the individual factorizable contributions of Eq. (64). The numerical values are correct up to power corrections of the order $\mathcal{O}(M_e/M_\mu)$ and arise from the diagram classes shown in Fig. 6.

Finally we convert the fine-structure constant in the perturbative expansion of the anomalous magnetic moment of the muon to the $\overline{\text{MS}}$ -scheme by using the conversion relations of Eqs.(28)-(37). As in the previous sections we consider here only the higher order QED corrections due to insertions of the electron vacuum polarization function into the leading order muon vertex diagram, as described in Section 1 and label the corresponding contribution to the anomalous magnetic moment with a_μ^{eVP} . Setting the scale to the mass of the muon we observe that all scale-dependend logarithms vanish and we obtain

$$\begin{aligned}
a_\mu^{\text{eVP}} = & \frac{\alpha_\mu}{2\pi} - \left(\frac{\alpha_\mu}{\pi}\right)^2 \frac{25}{36} + \left(\frac{\alpha_\mu}{\pi}\right)^3 \left(\frac{241}{2592} + \frac{\pi^2}{27} + \frac{\zeta_3}{2}\right) + \left(\frac{\alpha_\mu}{\pi}\right)^4 \left(\frac{253225}{93312} \right. \\
& - \frac{55}{648} \pi^2 - \frac{257}{144} \zeta_3 - \frac{5}{4} \zeta_5 \left. \right) - \left(\frac{\alpha_\mu}{\pi}\right)^5 \left(\frac{63114877}{6718464} + \frac{1361}{5832} \pi^2 \right. \\
& \left. - \frac{269}{17280} \pi^4 + \frac{1223}{5184} \zeta_3 - \frac{2}{9} \pi^2 \zeta_3 - \frac{4}{3} \zeta_3^2 - \frac{2795}{576} \zeta_5 - \frac{35}{8} \zeta_7 \right) + \mathcal{O}(\alpha_\mu^6), \quad (65)
\end{aligned}$$

with $\alpha_\mu = \bar{\alpha}(\mu = M_\mu)$. We have checked that this also holds at six-loop order, where the remaining scale-independent parts are not shown in Eq. (65) since they contain still unknown contributions, for example those which arise from the unknown constant C_5 of Eq. (60).

9 Summary and conclusion

We have computed analytically the vacuum polarization function at four-loop order in perturbative QED in the limit of small and large momentum, respectively. From the low energy limit we have derived the conversion factor of the fine structure constant between on-shell and $\overline{\text{MS}}$ scheme. These results have been used to derive analytical expressions for the dominant and gauge invariant contributions to the muon anomaly originating from vacuum polarization function insertions at five-loop order. Numerical results for these contributions are already available in the literature and are up to power corrections in agreement with our analytical ones.

Using the result of the recently computed five-loop QED β -function in the $\overline{\text{MS}}$ scheme of Ref. [1] we also determine the asymptotic momentum dependent part of the polarization function at five loops which in turn allows to calculate vacuum polarization type, asymptotic, leading contributions to the anomalous magnetic moment of the muon at six loops. The five-loop momentum dependent part of the polarization function is also used to determine the five-loop QED β -function in the on-shell scheme.

All the calculations described here were done during 2007-2008. A short version of this work, dealing only with the N=1 QED was reported at the 9th DESY Workshop on Elementary Particle Theory in the spring of 2008 [50].

Our results will be made available in computer readable form under the URL: <http://www-ttp.physik.uni-karlsruhe.de/Progdata/ttp12/ttp12-021> .

Acknowledgements

This work was supported by the Deutsche Forschungsgemeinschaft in the Sonderforschungsbereich/Transregio SFB/TR-9 “Computational Particle Physics” and by RFBR grants 11-02-01196, 10-02-00525. This work was also partially supported by U.S. Department of Energy under contract No.DE-AC02-98CH10886. The computer calculations were partially performed on the HP XC4000 supercomputer of the federal state Baden-Württemberg at the High Performance Computing Center Stuttgart (HLRS) under the grant “ParFORM”.

The figures have been drawn with the help of Axodraw [51] and JaxoDraw [52].

A $\overline{\text{MS}}$ -on-shell relation for fermion masses in QED

The relation between the $\overline{\text{MS}}$ -mass $\overline{m}(\mu)$ and the on-shell mass M for N identical fermions in QED is given by [42, 43]:

$$\begin{aligned}
\overline{m}(\mu) = M & \left(1 \right. \\
& + \left(\frac{\overline{\alpha}}{\pi} \right)^1 \left[-1 - \frac{3}{4} \ell_{\mu M} \right] \\
& + \left(\frac{\overline{\alpha}}{\pi} \right)^2 \left[\frac{7}{128} + \frac{143}{96} N - \frac{5}{16} \pi^2 - \frac{1}{6} N \pi^2 - \frac{3}{4} \zeta_3 + \frac{21}{32} \ell_{\mu M} \right. \\
& \quad \left. + \frac{13}{24} N \ell_{\mu M} + \frac{9}{32} \ell_{\mu M}^2 + \frac{1}{8} N \ell_{\mu M}^2 + \frac{1}{2} \pi^2 \ln(2) \right] \\
& + \left(\frac{\overline{\alpha}}{\pi} \right)^3 \left[-\frac{2969}{768} + \frac{1067}{576} N - \frac{9481}{7776} N^2 - \frac{613}{192} \pi^2 - \frac{85}{108} N \pi^2 + \frac{4}{135} N^2 \pi^2 \right. \\
& \quad - \frac{1}{48} \pi^4 + \frac{91}{2160} N \pi^4 - \frac{81}{16} \zeta_3 - \frac{53}{24} N \zeta_3 + \frac{11}{18} N^2 \zeta_3 - \frac{1}{16} \pi^2 \zeta_3 \\
& \quad + \frac{5}{8} \zeta_5 - \frac{489}{512} \ell_{\mu M} - \frac{151}{384} N \ell_{\mu M} - \frac{197}{216} N^2 \ell_{\mu M} + \frac{15}{64} \pi^2 \ell_{\mu M} + \frac{1}{3} N \pi^2 \ell_{\mu M} \\
& \quad + \frac{1}{9} N^2 \pi^2 \ell_{\mu M} + \frac{9}{16} \zeta_3 \ell_{\mu M} - \frac{1}{4} N \zeta_3 \ell_{\mu M} - \frac{27}{128} \ell_{\mu M}^2 - \frac{13}{32} N \ell_{\mu M}^2 \\
& \quad - \frac{13}{72} N^2 \ell_{\mu M}^2 - \frac{9}{128} \ell_{\mu M}^3 - \frac{3}{32} N \ell_{\mu M}^3 - \frac{1}{36} N^2 \ell_{\mu M}^3 + \frac{29}{4} \pi^2 \ln(2) \\
& \quad + \frac{8}{9} N \pi^2 \ln(2) - \frac{3}{8} \pi^2 \ell_{\mu M} \ln(2) - \frac{1}{3} N \pi^2 \ell_{\mu M} \ln(2) + \frac{1}{2} \pi^2 \ln^2(2) \\
& \quad \left. - \frac{1}{9} N \pi^2 \ln^2(2) - \frac{1}{2} \ln^4(2) + \frac{1}{9} N \ln^4(2) - 12 a_4 + \frac{8}{3} N a_4 \right], \tag{66}
\end{aligned}$$

with $\ell_{\mu M} = \ln(\mu^2/M^2)$.

References

- [1] P. Baikov, K. Chetyrkin, J. Kühn, and J. Rittinger, *Vector Correlator in Massless QCD at Order $O(\alpha_s^4)$ and the QED beta-function at five loop*, *JHEP* **1207** (2012) 017, [arXiv:1206.1284].
- [2] **Muon G-2** Collaboration, G. W. Bennett et al., *Final report of the muon E821 anomalous magnetic moment measurement at BNL*, *Phys. Rev.* **D73** (2006) 072003, [hep-ex/0602035].
- [3] **Particle Data Group** Collaboration, K. Nakamura et al., *Review of particle physics*, *J. Phys.* **G37** (2010) 075021.

- [4] T. Aoyama, M. Hayakawa, T. Kinoshita, and M. Nio, *Complete Tenth-Order QED Contribution to the Muon $g-2$* , *Phys. Rev. Lett.* **109** (2012) 111808, [[arXiv:1205.5370](#)].
- [5] K. Melnikov and A. Vainshtein, *Theory of the muon anomalous magnetic moment*, *Springer Tracts Mod. Phys.* **216** (2006) 1–178.
- [6] F. Jegerlehner, *The Anomalous Magnetic Moment of the Muon*, *Springer Tracts Mod. Phys.* **226** (2008) 1–426.
- [7] F. Jegerlehner and A. Nyffeler, *The Muon $g-2$* , *Phys. Rept.* **477** (2009) 1–110, [[arXiv:0902.3360](#)].
- [8] B. Lautrup and E. de Rafael, *The anomalous magnetic moment of the muon and short- distance behaviour of quantum electrodynamics*, *Nucl. Phys.* **B70** (1974) 317–350.
- [9] D. J. Broadhurst, A. L. Kataev, and O. V. Tarasov, *Analytical on-shell QED results: Three loop vacuum polarization, four loop Beta function and the muon anomaly*, *Phys. Lett.* **B298** (1993) 445–452, [[hep-ph/9210255](#)].
- [10] T. Kinoshita, H. Kawai, and Y. Okamoto, *Asymptotic photon propagator in massive QED and the muon anomalous magnetic moment*, *Phys. Lett.* **B254** (1991) 235–240.
- [11] P. A. Baikov and D. J. Broadhurst, *Three-loop QED vacuum polarization and the four-loop muon anomalous magnetic moment*, [hep-ph/9504398](#).
- [12] R. Barbieri and E. Remiddi, *Electron and Muon $1/2(g-2)$ from Vacuum Polarization Insertions*, *Nucl. Phys.* **B90** (1975) 233.
- [13] M. Nio, T. Aoyama, M. Hayakawa, and T. Kinoshita, *QED contributions to muon $g-2$: Tenth-order graphs*, *Nucl. Phys. Proc. Suppl.* **169** (2007) 238–243.
- [14] A. L. Kataev, *Renormalization group and the five loop QED asymptotic contributions to the muon anomaly*, *Phys. Lett.* **B284** (1992) 401–409; A. L. Kataev, *Phys. Lett.* **B710** (2012) 710 (Erratum).
- [15] S. Laporta, *Analytical and numerical contributions of some tenth order graphs containing vacuum polarization insertions to the muon ($g-2$) in QED*, *Phys. Lett.* **B328** (1994) 522–527, [[hep-ph/9404204](#)].
- [16] K. G. Chetyrkin, J. H. Kühn, and A. Kwiatkowski, *QCD corrections to the e^+e^- cross-section and the Z boson decay rate: Concepts and results*, *Phys. Rept.* **277** (1996) 189–281.
- [17] N. N. Bogolyubov and D. V. Shirkov, *Charge renormalization group in quantum field theory*, *Nuovo Cim.* **3** (1956) 845–863.

- [18] D. Shirkov, *The Bogolyubov renormalization group in theoretical and mathematical physics*, [hep-th/9903073](#).
- [19] J. A. M. Vermaseren, *New features of FORM*, [math-ph/0010025](#).
- [20] J. A. M. Vermaseren, *Tuning FORM with large calculations*, *Nucl. Phys. Proc. Suppl.* **116** (2003) 343–347, [[hep-ph/0211297](#)].
- [21] M. Tentyukov and J. A. M. Vermaseren, *Extension of the functionality of the symbolic program FORM by external software*, *Comput. Phys. Commun.* **176** (2007) 385–405, [[cs/0604052](#)].
- [22] P. Nogueira, *Automatic Feynman graph generation*, *J. Comput. Phys.* **105** (1993) 279–289.
- [23] P. A. Baikov, *A practical criterion of irreducibility of multi-loop Feynman integrals*, *Phys. Lett.* **B634** (2006) 325–329, [[hep-ph/0507053](#)].
- [24] P. A. Baikov, *Explicit solutions of the 3-loop vacuum integral recurrence relations*, *Phys. Lett.* **B385** (1996) 404–410, [[hep-ph/9603267](#)].
- [25] P. A. Baikov and K. G. Chetyrkin, *Four Loop Massless Propagators: an Algebraic Evaluation of All Master Integrals*, *Nucl. Phys.* **B837** (2010) 186–220, [[arXiv:1004.1153](#)].
- [26] R. N. Lee, A. V. Smirnov, and V. A. Smirnov, *Master Integrals for Four-Loop Massless Propagators up to Transcendentality Weight Twelve*, *Nucl. Phys.* **B856** (2012) 95–110, [[arXiv:1108.0732](#)].
- [27] S. Laporta and E. Remiddi, *The analytical value of the electron ($g-2$) at order α^3 in QED*, *Phys. Lett.* **B379** (1996) 283–291, [[hep-ph/9602417](#)].
- [28] S. Laporta, *High-precision calculation of multi-loop Feynman integrals by difference equations*, *Int. J. Mod. Phys.* **A15** (2000) 5087–5159, [[hep-ph/0102033](#)].
- [29] R. H. Lewis, *Fermat’s user guide*, *Fermat’s User Guide*, <http://www.bway.net/~lewis/>.
- [30] S. Laporta, *High-precision epsilon expansions of massive four-loop vacuum bubbles*, *Phys. Lett.* **B549** (2002) 115–122, [[hep-ph/0210336](#)].
- [31] K. Chetyrkin, J. H. Kühn, P. Mastrolia, and C. Sturm, *Heavy-quark vacuum polarization: First two moments of the $\mathcal{O}(\alpha_s^3 n_f^2)$ contribution*, *Eur. Phys. J.* **C40** (2005) 361–366, [[hep-ph/0412055](#)].
- [32] B. A. Kniehl and A. V. Kotikov, *Calculating four-loop tadpoles with one non-zero mass*, *Phys. Lett.* **B638** (2006) 531–537, [[hep-ph/0508238](#)].

- [33] Y. Schröder and A. Vuorinen, *High-precision epsilon expansions of single-mass-scale four-loop vacuum bubbles*, *JHEP* **0506** (2005) 051, [[hep-ph/0503209](#)].
- [34] Y. Schröder and M. Steinhauser, *Four-loop singlet contribution to the rho parameter*, *Phys. Lett.* **B622** (2005) 124–130, [[hep-ph/0504055](#)].
- [35] K. G. Chetyrkin, M. Faisst, C. Sturm, and M. Tentyukov, *ε -finite basis of master integrals for the integration-by-parts method*, *Nucl. Phys.* **B742** (2006) 208–229, [[hep-ph/0601165](#)].
- [36] E. Bejdakic and Y. Schröder, *Hypergeometric representation of a four-loop vacuum bubble*, *Nucl. Phys. Proc. Suppl.* **160** (2006) 155–159, [[hep-ph/0607006](#)].
- [37] B. A. Kniehl and A. V. Kotikov, *Heavy-quark QCD vacuum polarisation function: Analytical results at four loops*, *Phys. Lett.* **B642** (2006) 68–71, [[hep-ph/0607201](#)].
- [38] B. A. Kniehl, A. V. Kotikov, A. I. Onishchenko, and O. Veretin, *Strong-coupling constant with flavor thresholds at five loops in the \overline{MS} scheme*, *Phys. Rev. Lett.* **97** (2006) 042001, [[hep-ph/0607202](#)].
- [39] A. L. Kataev, *The comments on QED contributions to $(g-2)(\mu)$* , *hep-ph/0602098* (2006) [[hep-ph/0602098](#)].
- [40] A. Czarnecki and M. Skrzypek, *The Muon anomalous magnetic moment in QED: Three-loop electron and tau contributions*, *Phys. Lett.* **B449** (1999) 354–360, [[hep-ph/9812394](#)].
- [41] J.-P. Aguilar, D. Greynat, and E. de Rafael, *Muon Anomaly from Lepton Vacuum Polarization and The Mellin-Barnes Representation*, *Phys. Rev.* **D77** (2008) 093010, [[arXiv:0802.2618](#)].
- [42] K. Chetyrkin and M. Steinhauser, *The relation between the \overline{MS} and the on-shell quark mass at order α_s^3* , *Nucl. Phys.* **B573** (2000) 617–651, [[hep-ph/9911434](#)].
- [43] K. Melnikov and T. v. Ritbergen, *The three-loop relation between the \overline{MS} and the pole quark masses*, *Phys. Lett.* **B482** (2000) 99–108, [[hep-ph/9912391](#)].
- [44] E. de Rafael and J. Rosner, *Short-distance behavior of quantum electrodynamics and the Callan-Symanzik equation for the photon propagator*, *Annals Phys.* **82** (1974) 369–406.
- [45] T. Kinoshita and M. Nio, *The tenth-order QED contribution to the lepton $g-2$: Evaluation of dominant α^5 terms of muon $g-2$* , *Phys. Rev.* **D73** (2006) 053007, [[hep-ph/0512330](#)].

- [46] T. Aoyama, M. Hayakawa, T. Kinoshita, and M. Nio, *Tenth-Order Lepton Anomalous Magnetic Moment – Second- Order Vertex Containing Two Vacuum Polarization Subdiagrams, One Within the Other*, *Phys. Rev.* **D78** (2008) 113006, [[arXiv:0810.5208](#)].
- [47] T. Aoyama, M. Hayakawa, T. Kinoshita, and M. Nio, *Proper Eighth-Order Vacuum-Polarization Function and its Contribution to the Tenth-Order Lepton $g-2$* , *Phys. Rev.* **D83** (2011) 053003, [[arXiv:1012.5569](#)].
- [48] T. Aoyama, M. Hayakawa, T. Kinoshita, M. Nio, and N. Watanabe, *Eighth-Order Vacuum-Polarization Function Formed by Two Light-by-Light-Scattering Diagrams and its Contribution to the Tenth-Order Electron $g-2$* , *Phys. Rev.* **D78** (2008) 053005, [[arXiv:0806.3390](#)].
- [49] P. J. Mohr, B. N. Taylor, and D. B. Newell, *CODATA Recommended Values of the Fundamental Physical Constants: 2010*, [arXiv:1203.5425](#).
- [50] P. Baikov, K. Chetyrkin, and C. Sturm, *New Results in Four and Five Loop QED calculations*, *Nucl. Phys. Proc. Suppl.* **183** (2008) 8–13, [[arXiv:0807.1646](#)].
- [51] J. Vermaseren, *Axodraw*, *Comput. Phys. Commun.* **83** (1994) 45–58.
- [52] D. Binosi and L. Theussl, *JaxoDraw: A graphical user interface for drawing Feynman diagrams*, *Comput. Phys. Commun.* **161** (2004) 76–86, [[hep-ph/0309015](#)].